On the High-Order Multidimensional Gas-Kinetic Scheme

Qibing Li and Song Fu
Corresponding author: lqb@tsinghua.edu.cn

Department of Engineering Mechanics, Tsinghua University, Beijing 100084, China

Abstract: The newly developed high-order-accurate multidimensional gas-kinetic scheme is further investigated, including the benefit of the consideration of tangential slopes in the flux function at a cell interface, and the application of the scheme in turbulence simulation. The present study shows that in despite of increasing of computational cost, the multidimensional scheme can evidently improve the accuracy when compared to the directional splitting one. The numerical simulation of the compressible turbulence with the high-order multidimensional gas-kinetic scheme shows better performance than the existing second-order gas-kinetic method.

Keywords: High-Order Gas-Kinetic Scheme, Multidimensional Method, Compressible Turbulence.

1   Introduction

The foundation for the development of modern compressible flow solver is the Riemann solution of the inviscid Euler equations. However, due to the lack of a multidimensional Riemann solution, it is also a great challenge to construct a genuinely multidimensional scheme. An alternative approach to develop a CFD scheme is based on the gas-kinetic theory, such as the multidimensional BGK-NS flow solver [1, 2], which has shown good performance in many flow fields. The success comes from the fact that the kinetic equation has the mechanism to accurately describe the gas evolution starting from an initial discontinuous data, including the inherent multidimensional characteristics of the particle transport. Recently, through the high-order expansion of equilibrium distribution function the high-order multidimensional gas-kinetic BGK scheme (HGKS or HBGK) has been successfully developed [3, 4], which puts a new way to construct high-order-accurate truly multidimensional scheme for compressible flows.

In the present study, the difference in performance among the multidimensional (MD) third-order gas-kinetic scheme, the corresponding quasi-one-dimensional (Q1D) extension and the directional (DS) scheme are investigated for both viscous and inviscid flows.

2   High-Order Gas-Kinetic Scheme

The construction of gas-kinetic BGK scheme [1] is briefly described as follows. First, the BGK-Boltzmann equation for three-dimensional (3-D) flow is written as

$$\frac{\partial f}{\partial t} + \mathbf{u} \cdot \frac{\partial f}{\partial \mathbf{x}} = \frac{g - f}{\tau} , \qquad (1)$$

where f is the gas distribution function at a point in phase space $(\mathbf{x}, \mathbf{u}, t, \xi)$ and $\tau = \mu/p$ is the collision time. g is the local equilibrium state of the gas approached by f,

$$g = \rho(\lambda/\pi)^{(K+2)/2} e^{-\lambda[(\mathbf{u}-\mathbf{U})^2 + \xi^2]}, \tag{2}$$

with $\lambda = 1/(2RT)$ and the total number of degrees of freedom $K = (5 - 3\gamma)/(\gamma - 1)$. During the particle collisions, f and g satisfy the conservation constraint,

$$\int \psi_\alpha (f - g) d\Xi = 0, \quad \alpha = 1-5, \tag{3}$$

at any point in space and time for the conservation of mass, momentum and energy. Here $d\Xi = d\mathbf{u}d\xi$ is the volume element in the phase space and $\psi = (1, \mathbf{u}, (\mathbf{u}^2 + \xi^2)/2)^T$ is the vector of moments.

Thus the finite-volume method can be constructed as

$$(\mathbf{Q}*)_{ijk}^{n+1} = (\mathbf{Q}*)_{ijk}^n + \frac{1}{V_{ijk}} \oiint_{S_{ijk}} \int_{t^n}^{t^n + \Delta t} \mathbf{F} * dt d\mathbf{S} . \tag{4}$$

The superscript `*' represents the variable in the global coordinates. The flux $\mathbf{F}*$ is calculated through the transformation from that in the local coordinates $\mathbf{F}$. The relations between f and the macroscopic conservative quantities $\mathbf{Q}$ and the flux $\mathbf{F}$ are given by

$$\mathbf{Q} = (\rho, \rho\mathbf{U}, \rho E)^T = \int f\psi d\Xi \tag{5}$$

$$\mathbf{F}* = (F_1, n_{1\beta}F_\beta, n_{2\beta}F_\beta, n_{3\beta}F_\beta, F_5)^T, \quad \beta = 2,3,4$$
$$F_\alpha = \int u f \psi_\alpha d\Xi, \quad \alpha = 1-5. \tag{6}$$

The BGK equation (1) has the integral solution for constant collision time τ,

$$f(\mathbf{x}, t, \mathbf{u}, \xi) = \frac{1}{\tau} \int_0^t g(\mathbf{x}', t', \mathbf{u}, \xi) e^{-(t-t')/\tau} dt' + e^{-t/\tau} f_0(\mathbf{x} - \mathbf{u}t), \tag{7}$$

where $\mathbf{x}' = \mathbf{x} - \mathbf{u}(t - t')$ is the trajectory of a particle motion and f_0 is the initial gas distribution function at the beginning of each time step ($t = 0$).

If f_0 and g is known, the time dependent distribution function f can be easily deduced through the above expression, avoiding the great difficulty to solve the BGK equation directly. This is adopted by the gas-kinetic scheme, with the key to construct f_0 and g around the cell interface according to the Chapman-Enskog expansion. Details can be found in references [1].

In order to develop a high-order accurate gas-kinetic BGK scheme, we can construct the high-order accurate initial distribution function f_0 and the equilibrium distribution g through the expansion to third-order in both spatial and temporal directions. The genuinely multidimensional scheme can be constructed with the following f_0 and g, including both the normal and tangential slopes,

$$f_0(\mathbf{x}, 0, \mathbf{u}, \xi)$$
$$= g^l \left(1 + a_i^l x_i - \tau(a_i^l u_i + A^l) - \tau(a_i^l A^l + C_i^l)x_i + (a_i^l a_j^l + b_{ij}^l)(-\tau u_i x_j + x_i x_j/2)\right)(1 - H[x_1]) \tag{8}$$
$$+ g^r \left(1 + a_i^r x_i - \tau(a_i^r u_i + A^r) - \tau(a_i^r A^r + C_i^r)x_i + (a_i^r a_j^r + b_{ij}^r)(-\tau u_i x_j + x_i x_j/2)\right)H[x_1]$$

$$g(\mathbf{x}, t, \mathbf{u}, \xi) = g_0\left(1 + a_i x_i + At + (a_i a_j + b_{ij})x_i x_j/2 + (C_i + Aa_i)x_i t + (A^2 + B')t^2/2\right) \tag{9}$$

where g_0 is the initial local Maxwellians and H is the Heaviside function. The local terms a_i, b_{ij}, C_i, B' and A are from the Taylor expansion of a Maxwellian and take the form, $a = a^{(\alpha)}\psi_\alpha, \alpha = 1-5$, where all coefficients are local constants from the first and second derivatives of g and can be determined by are the reconstructed conservative variables $\mathbf{Q}$ and their slopes. Then the distribution function at the cell interface can be deduced,

$$
\begin{aligned}
f(0, x_2, x_3, \mathbf{u}, t) = &(1-D)g_0 + (-\tau + (t+\tau)D)a_k u_k g_0 + (t - \tau + \tau D)A g_0 \\
&+ (1-D)\left((a_2^2 + b_{22})x_2^2/2 + (a_3^2 + b_{33})x_3^2/2\right)g_0 \\
&+ \left(\tau^2(1-D) - (t^2/2 + \tau t)D\right)\left((a_m a_n + b_{mn})u_m u_n\right)g_0 \\
&+ \left(t^2/2 - \tau t + \tau^2(1-D)\right)(A^2 + B')g_0 \\
&+ \left(2\tau^2(1-D) - \tau t(1+D)\right)(C_k + A a_k)u_k g_0 \\
&+ D\left[\begin{pmatrix} 1 - (t+\tau)a_k^l u_k - \tau A^l + \tau t(A^l a_k^l + C_k^l)u_k \\ + (\tau t + t^2/2)(a_m^l a_n^l + b_{mn}^l)u_m u_n \\ + ((a_2^l)^2 + b_{22}^l)x_2^2/2 + ((a_3^l)^2 + b_{33}^l)x_3^2/2 \end{pmatrix} H(u_1)g^l \right. \\
&\left. + \begin{pmatrix} 1 - (t+\tau)a_k^r u_k - \tau A^r + \tau t(A^r a_k^r + C_k^r)u_k \\ + (\tau t + t^2/2)(a_m^r a_n^r + b_{mn}^r)u_m u_n \\ + ((a_2^r)^2 + b_{22}^r)x_2^2/2 + ((a_3^r)^2 + b_{33}^r)x_3^2/2 \end{pmatrix}(1 - H(u_1))g^r \right] \quad (10)
\end{aligned}
$$

In the above equation, $D = e^{-t/\tau}$ and the variation of f along the tangential direction of the cell interface x_2, x_3 is represented through the tangential slopes, such as a_2, b_{12}, b_{22}, et al. However, the terms explicitly in proportion to x_2, x_3 are omitted, as the integration is zero. The terms containing x_2^2, x_3^2 are retained, which is necessary for the scheme to achieve the third-order accuracy with only ONE integral point (the center of the cell interface). Furthermore, the above solution allows the movement of particles in any direction. That is, the present high-order-accurate scheme simulates a multidimensional transport process across a cell interface. Thus it is a truly multidimensional scheme. However, if omit these coefficients related to tangential slopes, the corresponding quasi-one-dimensional (Q1D) extension and the directional (DS) scheme can be obtained.

It should be noted that the solution of BGK equation (7) has no specific requirement on the smoothness of the reconstructed initial data. That is, it can describe the flow evolution when $t < \tau$, which is not valid for the method based on Euler equations. Another point is that it is difficult to achieve high-order reconstruction of macro conservative variables for multidimensional flow. In the present study, the least-square method is adopted and the coefficients can be calculated in advance for only one time to decrease the computational cost. The 2nd-order PFGM limiter [5] is used mostly for the direct reconstruction of conservative variables when the flow contains discontinuities.

3 Numerical Results

The first test case is the isentropic vortex problem, with initial flow field $\rho = 1, p = 1, u = v = 1$ and perturbation $(\delta u, \delta v) = \varepsilon \exp[(1 - r^2)(-y, x)/2]$, $\delta T = (\gamma - 1)\varepsilon^2/(2\gamma)\exp[1 - r^2]$, $\delta S = 0$ and $\varepsilon = 5/(2\pi)$. The computational domain is $[-5, 5] \times [-5, 5]$ divided by uniform cells. Periodic boundary conditions are adopted. The computed error variations with different cell sizes are shown in figure 1, where the benefit of the including of tangential slopes in the flux function at a cell interface
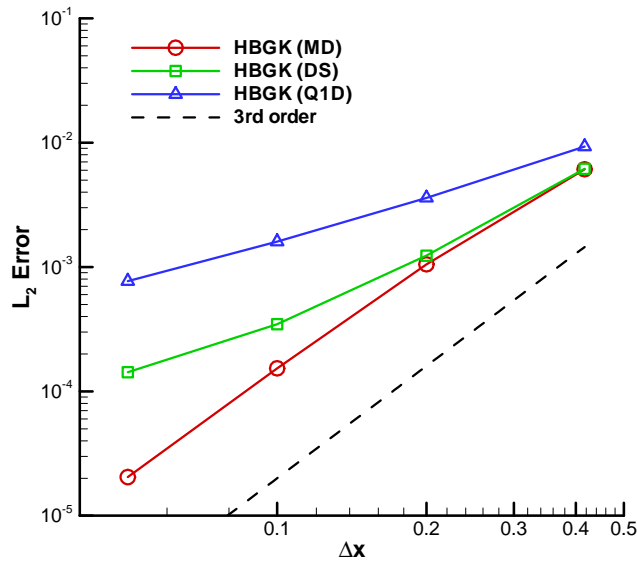
is evident.

Figure 1: Errors in density vs. cell size for isentropic vortex problem

The second case is a flat plate boundary layer flow with Mach number 0.15 and Reynolds number $\mathrm{Re}_L = 10^5, L = 100, U = 1$. The computational domain is chosen as $[-40, 100] \times [0, 50]$ and 120×30 grid cells are adopted with 40×30 cells locate ahead of the plate. The minimal cell sizes are $\Delta x_{\min} = 0.1, \Delta y_{\min} = 0.07$ with stretching rate $r_y = \Delta y_{j+1} / \Delta y_j = 1.18$. Figure 2 shows the velocity profiles at different streamwise locations. One can see that the velocity distributions, not only for the streamwise component, but also for the transverse one, can be accurately predicted with only four cells, which shows the good performance of the present scheme in viscous flow. In this case, the difference between the multidimensional scheme and the directional splitting one is not evident. It should be noted that for this small transverse stretching rate of the computational cell, the second-order reconstruction can give very good results. However, if increasing the stretching rate, $r_y = 1.27$, the third-order reconstruction can yield better transverse velocity profiles, especially near the outer edge of the boundary layer (see figure 3).
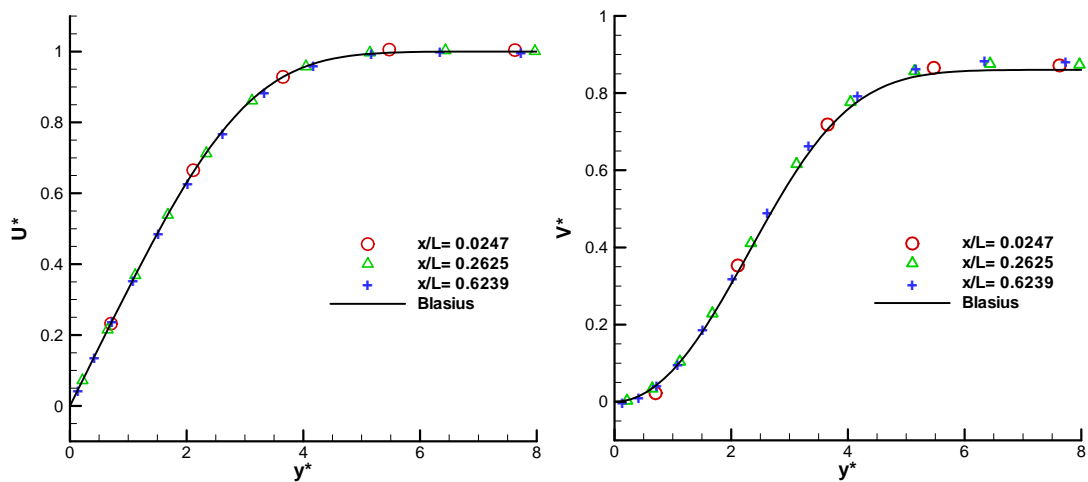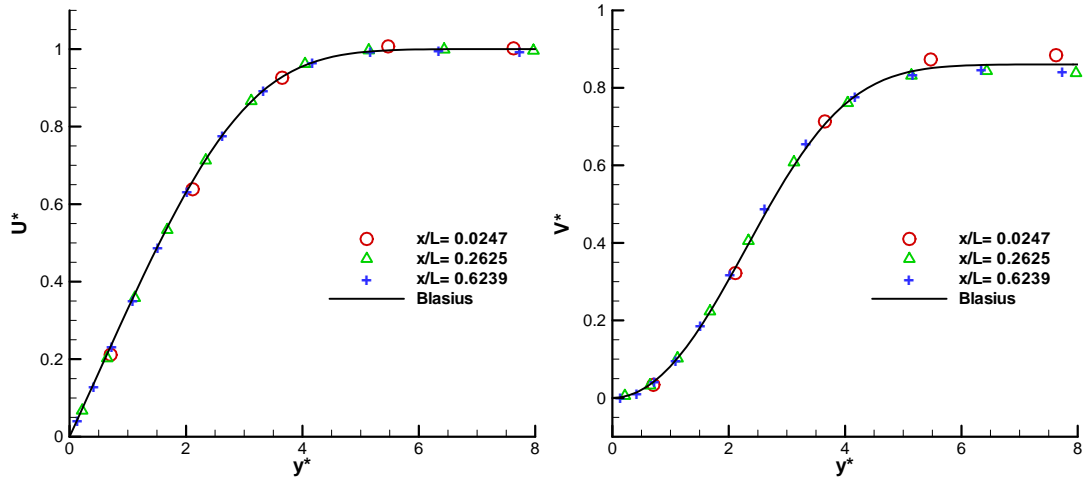
Figure 2: Streamwise and transverse velocity profiles at different streamwise locations. The top two figures are computed with MD-HBGK and the bottom DS-HBGK.
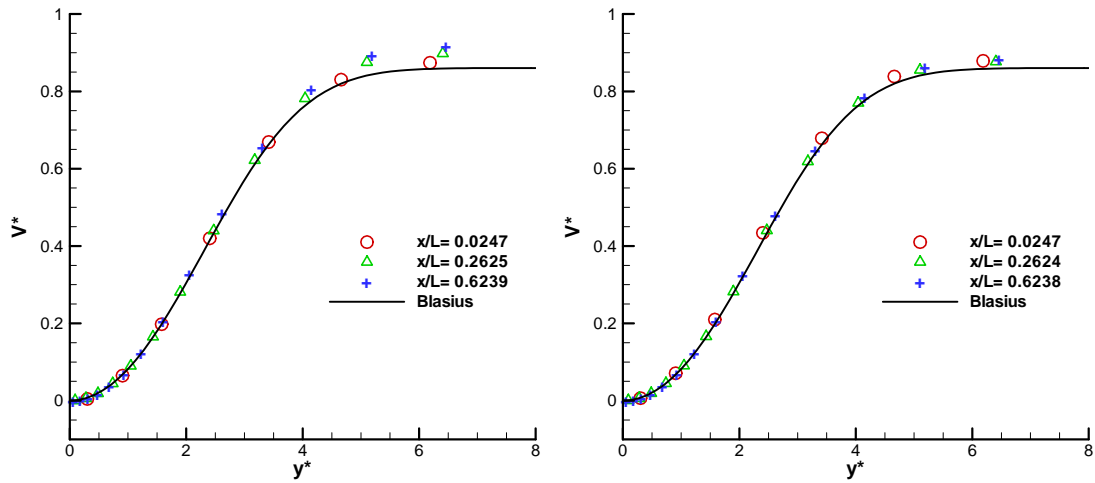

Figure 3: Transverse velocity profiles at different streamwise locations predicted with MD-HBGK. The left figure is for the second-order reconstruction and right the third-order.

The three-dimensional scheme is then developed and applied into the numerical simulation of compressible turbulence. Figure 4 shows the computed Mach number iso-surface for the isotropic turbulence with turbulent Mach number $M_t = 0.5$ and Reynolds number $\mathrm{Re}_\lambda = 72$. Uniform grid with 128^3 cells is adopted. The results show better performance of HBGK than the existing second-order gas-kinetic BGK method.
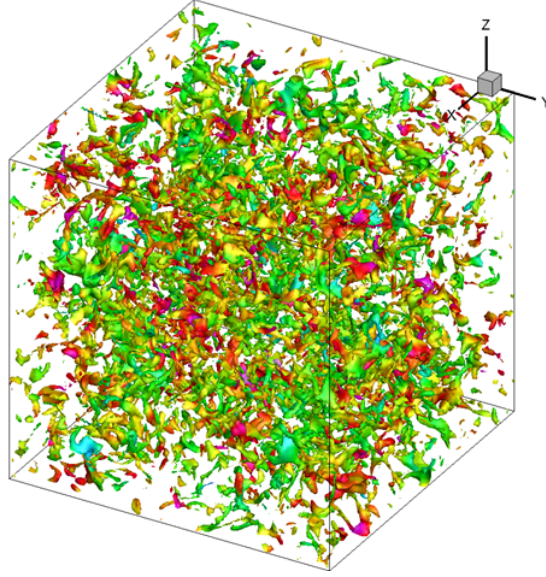
Figure 4: Mach number distribution in isotropic turbulence (iso-surface for $M = 0.05$ and color for pressure).
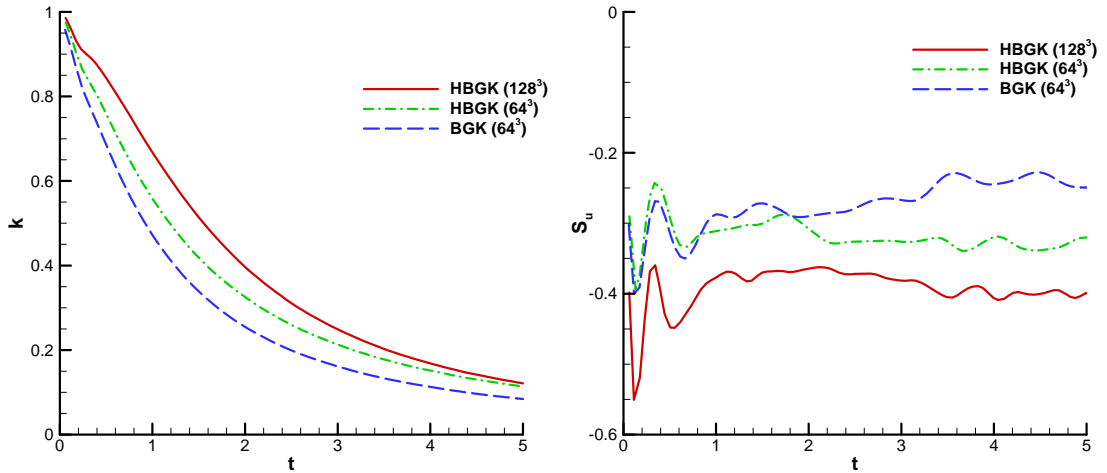

Figure 5: Histories of turbulent energies and streamwise skewness factors isotropic turbulence.

4 Conclusion and Future Work

In the present study, the construction of a high-order truly three-dimensional gas-kinetic scheme is introduced and the benefit of the consideration of tangential slopes in the flux function at a cell interface is investigated. In despite of increasing of computational cost, the multidimensional scheme can evidently improve the accuracy when compared to the directional splitting one. The numerical simulation of the compressible isotropic turbulence with the high-order multidimensional gas-kinetic scheme shows better performance than the existing second-order gas-kinetic BGK method. The effect of the limiter for reconstruction requires further study.

Acknowledgements

References

[1] K. Xu. A gas-kinetic BGK scheme for the Navier-Stokes equations, and its connection with artificial dissipation and Godunov method. J. Comput. Phys., 171:289, 2001.

[2] Q.B. Li, S. Fu. On the multidimensional gas-kinetic BGK scheme, J. Comput. Phys., 220:532-548, 2006

[3] Q.B. Li, K. Xu, S. Fu. A high-order gas-kinetic Navier-Stokes flow solver, J. Comput. Phys., 229:6715-6731, 2010.

[4] Q.B. Li, K. Xu, S. Fu. A new high-order multidimensional scheme, Computational Fluid Dynamics 2010: Proceedings of the Sixth International Conference on Computational Fluid Dynamics, ICCFD6, St Petersburg, Russia.

[5] M. Yang, Z.J. Wang. A parameter-free generalized moment limiter for high-order methods on unstructured grids. Adv. Appl. Math. Mech., 4, 451–480, 2009.